Installation and Validation of MCNP-4A

Ansto

nuclear technology

NTD/TN 200

AUSTRALIAN NUCLEAR SCIENCE
AND TECHNOLOGY ORGANISATION

LUCAS HEIGHTS RESEARCH LABORATORIES

Installation and Validation of MCNP-4A

by

N. A. Marks

January, 1997

1 INTRODUCTION

MCNP-4A [1] is a multi-purpose Monte Carlo program suitable for the modelling of neutron, photon, and electron transport problems. It is a particularly useful technique when studying systems containing irregular shapes. MCNP has been developed over the last 25 years by Los Alamos, and is distributed internationally via RSIC at Oak Ridge.

This document describes the installation of MCNP-4A (henceforth referred to as MCNP) on the Silicon Graphics workstation *bluey.ansto.gov.au*. A limited number of benchmarks pertaining to fast and thermal systems were performed to check the installation and validate the code. The results are compared to deterministic calculations performed using the AUS neutronics code system [2] developed at ANSTO.

2 INSTALLATION and USAGE

MCNP is installed on the SGi workstation *bluey* and is also available on *pion* by way of a symbolic link. The main directory is `nigel/mcnp`, which contains the MCNP executable as well as several utility programs for managing cross-section files and MCNP input/output. Binary versions of the cross-section files are stored in `nigel/mcnp/lib`. An archive of the MCNP distribution extracted from the exabyte tapes is stored on *pupil* in the directory `gsr/nigel-mcnp`. The original ascii versions of the cross-section files can also be found within this directory.

The file `gsr/nucanl/mcnp` is a symbolic link which points to the MCNP executable. Since the typical user will already have `gsr/nucanl` in their PATH, they are able to use MCNP immediately, with no setup required. Typing `mcnp inp=inputfile` at the command line will run MCNP and write the output files to the current directory. A user wishing to make use of extra utilities available in the MCNP directory would need to add `nigel/mcnp` to their PATH.

The utilities available in `nigel/mcnp` include the `makxsf` program which comes with the MCNP distribution, and two locally written scripts, `isotope` and `ratio`. A brief description of the three utilities is given below.

- `makxsf` is used to manipulate the form and structure of the cross-section libraries. Its uses include the creation of problem specific cross-section libraries and the conversion of libraries between ascii and binary forms. Instructions on the usage of `makxsf` can be found in the MCNP manual.

- The ENDF/B-VI library distributed with MCNP does not contain cross-sections for natural abundances of many common elements, such as iron, copper and nickel. Consequently, the input file must specify all of the naturally occurring isotopes of the required element. This process is both prone to error and time consuming. The script `isotope` provides a simple method of producing the MCNP input for a desired material. At the command line the user types the keyword `isotope` followed by the chemical symbol for the element and the amount of the element. The amount can be either a percentage fraction or in units of atom/barn-cm, as the script produces two sets of output suitable suitable for either form of input. For example,

`isotope fe 0.1` would produce the MCNP input for natural iron at a concentration of 0.1% *and* 0.1 atoms/barn-cm. For convenience `isotope` is also available to the general user via a symbolic link in `gsr/nucanl`.

- The script `ratio` was written to assist in the analysis of the reaction rates in the benchmarks. Calculation of the reaction rates and the subsequent comparison with experiment is a tedious process and prone to error. The script automates this process by reading the MCNP output file, calculating the required quantities, and comparing them to the experiment values. A typical invocation of ratio would read `ratio fast godiva output`, where `fast` denotes a fast neutron system, `godiva` refers to the experimental data, and `output` is the MCNP output file. The full range of options can be found be viewing the directory `nigel/mcnp/scripts/ratio`.

2.1 Installation Details

The installation of MCNP was reasonably straightforward, although a few difficulties had to be overcome. The first problem concerned the data on the RSIC exabyte tapes. The distribution documentation did not say which data format (`/dev/tape`, `/dev/tapens`, `/dev/nrtape` or `/dev/nrtapens`) had been used to write to the tapes. Trial and error revealed that `/dev/tapens` was the correct format. The several tarfiles which comprise the MCNP distribution were then extracted using the command

```
tar xvf /dev/tapens filename.tar.Z
```

The second and third problems concerned the compilation stage, where it was found that the compilation flags supplied for the SGi produced compilation and run-time errors. To correct these errors it was necessary to modify the file `mcsetup.for` and change the compile options on line 360 from

```
f77 -O2 -Olimit 1500 -Nn2000 -Nq1000 -Ns1000 -Nx1000
```

to

```
f77 -O1 -Olimit 1500 -Nn6000 -Nq6000 -Ns6000 -Nx2000
```

If the -N*xyyyy* options were used as supplied, the compilation would fail. The new values of these options were taken from the SunOS compilation options on line 379 of `mcsetup.for`. When these values were used the compilation was successful. However, when the MCNP test cases were run, runtime errors occurred due to problems related to DXTRAN spheres. This was a curious error as the majority of the test cases do not contain any references to DXTRAN spheres. The problem disappeared when the optimisation flag was changed from `-O2` to `-O1`. With this change the test cases ran successfully and the installation was complete.

2.2 Cross section files

The cross section files can be found in the directory `mcnp/lib`. This directory contains the cross section data for neutrons, photons and electrons, although the vast majority of the 85 megabytes of data constists of neutron cross sections. The electron data can be found in the file `el1`, while the photon data is in the files `mcplib1` and `mcplib02`.

The neutron data includes the unreleased ENDF/B-V data, as well as ENDFB/-IV and earlier files. The format of the new ENDF/B-VI cross sections is different to the earlier data due to the vast increase in size of the ENDF-B/VI cross section files. In ENDF-B/V and earlier data, each cross section file was a library of a large number of isotopes. These isotope cross sections were concatenated into a single file, which could be up to 8 megabytes in size. The size of the ENDF/B-VI data files however, precluded this approach, as the typical size of the cross section file for individual isotopes was 0.5 megabyte. The approach taken by the developers of MCNP was to store the ENDF-B/VI data in a separate file for each isotope. The naming scheme used for these files is a five to seven character word containing, in order, the chemical symbol of the isotope, the atomic number, and the atomic weight. Some examples of this naming convention are `h1001`, `he2003` and `u92235`.

Within the cross section index file `xsdir`, these ENDF/B-VI data files are referred to using the suffix `.60c` and the chemical symbol is absent. Within `xsdir` the ENDF/B-VI files are the default cross sections, unless overridden explicitly by appending a suffix to indicate the desired data set. If the user desires default cross sections different to those in `mcnp/lib/xsdir`, the MCNP utility `makxsf` can be used.

All the cross sections were converted from ascii to binary format to save disk space. An automated script was written around `makxsf` to read in the ascii files, write them out as binary files under a different name, and then write the binary file back over the original ascii file. This script can be found in the directory `nigel/mcnp/lib/convert`. The original ascii files can be found on *pupil* in the directory `gsr/nigel-mcnp/lib/ascii`. It is interesting to note that no noticeable speedup in calculation speed was found with the binary files. This reflects the use of dynamic memory allocation in MCNP, reducing the need for I/O access.

3 BENCHMARKS

A series of benchmark calculations were performed to validate the installation and to provide a comparison between MCNP and the locally developed AUS neutronics code. While both codes are based on ENDF/B-VI data, the AUS system uses a deterministic approach in contrast to the Monte Carlo algorithm employed by MCNP. A series of fast and thermal assemblies were calculated, examining both uranium and plutonium systems. The AUS results are taken from [3] which provides a comprehensive validation of the AUS code using the ENDF/B-VI library.

3.1 Thermal Reactor Assemblies

3.1.1 Homogeneous ^{235}U-H_2O benchmarks

The ORNL series of benchmarks consists of five unreflected spheres of ^{235}U (as uranyl nitrate) in H_2O, three of which were poisoned with boron. These benchmarks are useful for testing H_2O fast scattering data, and the ^{235}U and thermal absorption of hydrogen. The MCNP calculations used the model description as described in ENDF-202 [4]. A total of 1.26 million neutron histories were followed, reducing the uncertainty in the criticality constant to less than 0.0006 (one standard deviation). The input and output files can be found in the directories `nigel/mcnp/bench/ornl[1-4,10]`.

Figure 1 presents a graphical comparison of the AUS and MCNP calculations. Two features in particular are evident. The first is that both schemes slightly underestimate k-effective, and the second is that the two calculations are offset by a near-constant amount. The regular nature of the variation demonstrates the difference is not a statistical effect

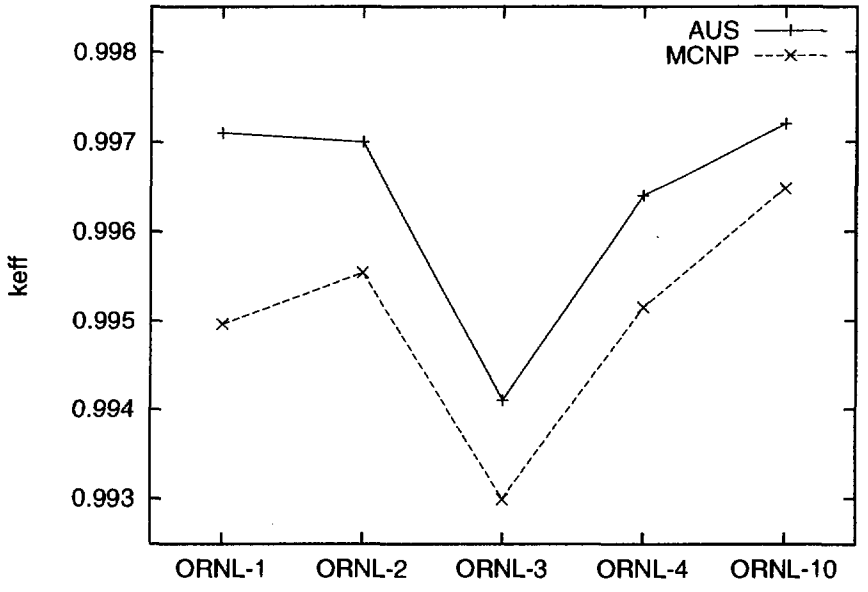

Figure 1: Criticality constant k_{eff} for the ORNL benchmarks as calculated using MCNP and AUS. The one standard deviation uncertainty for the MCNP values is less than 0.0006.

Assembly	AUS	MCNP	Difference
ORNL-1	0.9971	0.9950	-0.0021
ORNL-2	0.9970	0.9955	-0.0015
ORNL-3	0.9941	0.9930	-0.0011
ORNL-4	0.9964	0.9952	-0.0012
ORNL-10	0.9972	0.9965	-0.0013
Average	0.9964	0.9950	-0.0014

Table 1: Criticality constant k_{eff} for the ORNL benchmark spheres. The standard deviation uncertainty is less than 0.0006.

due to Monte Carlo uncertainty, but instead is a true systematic offset. Several of the other benchmark calculations exhibit similar offsets between the AUS and MCNP calculations. While it is not clear what is producing this offset, differences in the pre-processing of the cross-section data provide the most likely explanation. Table 1 provides a numerical listing of the data in Figure 1. The Table also lists the difference in k_{eff} between MCNP and AUS, indicating an average difference of 0.14%.

3.1.2 Homogeneous ^{239}Pu-H_2O benchmarks

The PNL series of benchmarks consists of homogeneous aqueous solutions of plutonium nitrate with a broad range of hydrogen/Pu-239 ratios, as shown in Table 2. The MCNP calculations used the model specification described in ENDF-202 [4]. Where different specifications for an particular benchmark existed, the model used in the AUS calculation [3] was chosen. A total of 2.4 million neutron histories were followed, giving a one standard deviation uncertainty in k_{eff} of 0.0006. The input and output files can be found in the directories `nigel/mcnp/bench/pnl[6-11]`.

Table 2 presents a comparison between the MCNP and AUS calculations. Note that PNL-10 and PNL-11 the calculation was performed using the Monte Carlo code KENO V.a

Assembly	H/Pu (fissile)	AUS/KENO	MCNP	Difference
PNL-6B	131	1.0015	0.9980	-0.0035
PNL-7A	985	1.0063	1.0041	-0.0022
PNL-8A	795	1.0078	1.0037	-0.0041
PNL-9	953	0.9923	0.9928	0.0005
PNL-10	229	0.9999	0.9974	-0.0025
PNL-11	1192	1.0022	1.0005	-0.0017
Average		1.0017	0.9994	-0.0023

Table 2: Criticality constant k_{eff} for the PNL benchmarks. The standard deviation uncertainty in the MCNP values is 0.0006.

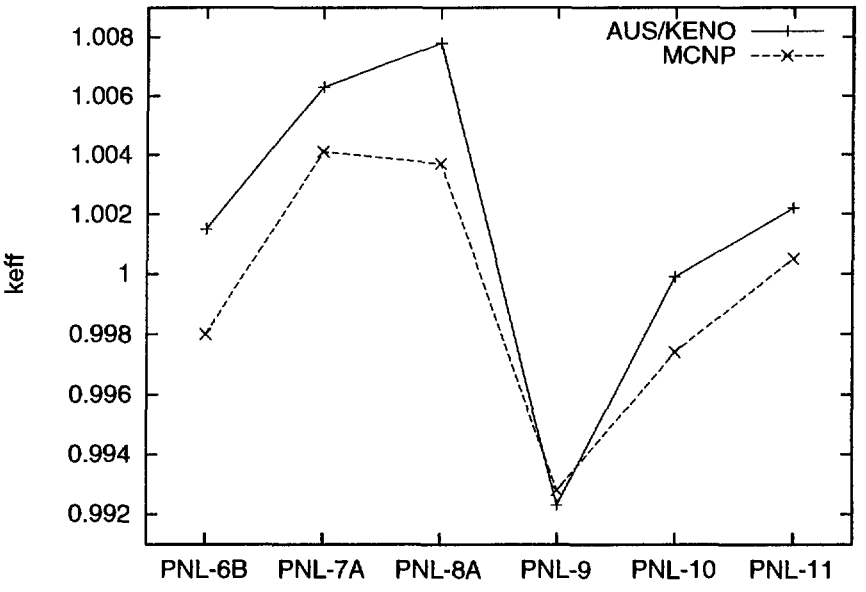

Figure 2: Criticality constant k_{eff} for homogeneous PNL criticals.

[5]. Figure 2 shows a graphical representation of the data in this Table. With the exception of PNL-9, the same systematic offset between MCNP and AUS seen in the ORNL benchmarks is present. The average difference in k_{eff} between the two methods is 0.23%, slightly higher than the ^{235}U ORNL spheres where the difference was 0.14%.

3.1.3 Light water moderated benchmark lattices

The TRX and BAPL series of benchmarks are similar in a number of respects. Both sets of assemblies are H_2O moderated, fully reflected and use uranium enriched to 1.3%. The major difference is in the composition of the fuel, which is pure uranium in the TRX lattices, and UO_2 in the BAPL lattices. This report presents calculations of the TRX-1,2 and BAPL-1,2 assemblies only.

The MCNP calculations of the TRX-1,2 lattices used a one-sixth core model with reflective boundaries. The dimensions and material composition were taken from ENDF-202 [4]. A total of 2.4 million neutron histories were followed, giving a one standard deviation uncertainty of 0.0004 in k_{eff}, and 0.005 in the reaction rates. The input and output files can be found in the directories `nigel/mcnp/bench/trx[1,2]`.

The reaction rates, which are defined in Table 4, were calculated over a central section of the core. This tally region measured 30 cm high and in cross-section consisted of a hexagonal area measuring 20.33 cm between opposing sides. This extended tally region introduced an error in the reaction rate of less than 0.1%. Figure 3 shows the radial variation in ρ^{28} in an AUS calculation of the TRX-1 lattice. Over the first five mesh points, a distance of 10.21 cm, the reaction rate varies by 0.0007, a fractional change of just 0.05%. The other reaction rates showed similarly small deviations.

The BAPL reaction rates and k_{eff} could not be calculated directly with MCNP as the specifications in ENDF-202 provide the buckling but not the dimensions of the core. The

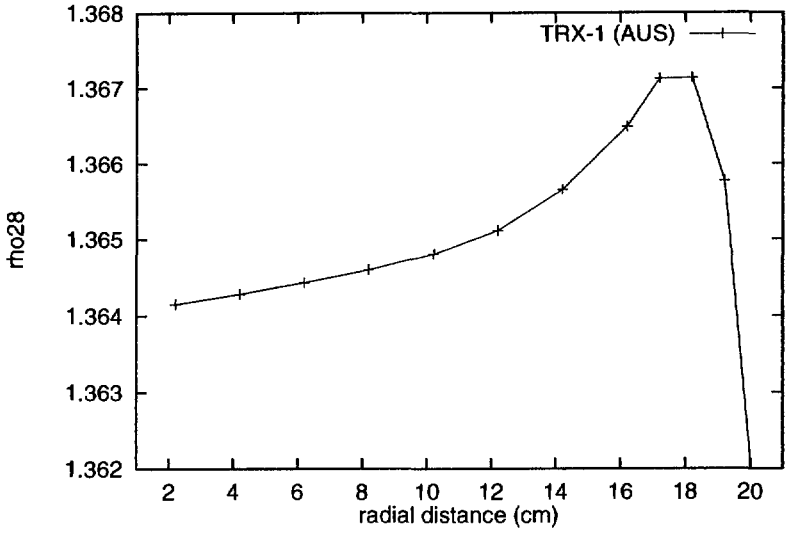

Figure 3: Radial variation of the reaction rate ρ^{28} in the central part of the TRX-1 core. The calculation was performed using the AUS neutronics scheme.

solution to this problem was to use MCNP to calculate k_{eff} and the reaction rates for an infinite system, and then scale the results using an AUS calculation. For example, the MCNP k_{eff} was computed using the formula

$$k_{\text{eff}}(\text{MCNP}) = \frac{k_\infty(\text{MCNP})}{k_\infty(\text{AUS})} \times k_{\text{eff}}(\text{AUS}), \tag{1}$$

where k_∞ denotes the neutron multiplication factor of the infinite system. Corresponding expressions were used to compute the reaction rates. This formula is appropriate only if MCNP and AUS predict the same fractional difference between infinite and finite assemblies. Table 3, which lists the results of a calculation of the TRX-1 assembly, shows that this is indeed the case. It is evident that the scaling algorithm produces an error in k_{eff} of just 0.06%, and three of the four reaction rates are accurate to within 0.4%. The fourth

	k_{eff}	ρ^{28}	δ^{25}	δ^{28}	C*
MCNP-infinite	1.1782	1.329	0.0965	0.0924	0.792
MCNP-reactor	0.9892	1.367	0.0995	0.1008	0.803
Ratio (inf/reactor)	1.1911	0.972	0.970	0.917	0.986
AUS-infinite	1.1805	1.320	0.0967	0.0905	0.786
AUS-reactor	0.9916	1.364	0.0995	0.0975	0.799
Ratio (inf/reactor)	1.1905	0.968	0.972	0.928	0.984
Difference	0.0006	0.004	-0.002	-0.011	0.002

Table 3: Calculations of the TRX-1 lattice to test the scaling algorithm used to infer k_{eff} and reaction rates for BAPL-1,2.

quantity, δ^{28}, for which the experimental error is typically 5%, is accurate to within 1%. It should also be noted that the MCNP values in Table 3 are subject to the statistical uncertainty recorded earlier. The k_∞ calculations of the BAPL lattices followed 2.4 million neutron histories. The input and output files for the calculations can be found in the directories `nigel/mcnp/bench/bapl[1,2]`.

Figure 4 shows the variation in k_{eff} for the four light water lattices. As in the previous benchmarks the MCNP value of k_{eff} is consistently several tenths of a percent below the AUS value. The average difference between the two sets of data is 0.27%, slightly higher than the offset found in the ^{235}U ORNL benchmarks. It is also evident that both MCNP and AUS underestimate k_{eff} by up to 1%. Further comment on this difference is made below. It should be noted that the TRX/AUS results quoted here use a radial model, in contrast to [3] where a cell calculation is reported. The radial model is used to provide a equivalent comparison with MCNP, as MCNP cannot make use of a buckling.

Figure 5 shows the reaction rates ρ^{28}, δ^{25} and δ^{28} for the four benchmarks. Relative to AUS, MCNP overestimates ρ^{28} and δ^{28}, but no trend is apparent for δ^{25}. The tendency for MCNP to predict higher values for ρ^{28} and δ^{28} than AUS is consistent with the lower value of k_{eff}. Higher values of ρ^{28} and δ^{28} indicate more epithermal ^{238}U captures and fewer ^{235}U fissions, both of which would act to lower k_{eff}. Since δ^{28} is sensitive to variations in the fast neutron spectrum, this data suggests that MCNP and AUS differ in their treatment of fast neutrons.

The three graphs in Figure 5 indicate varying behaviour of the quantities when compared to experiment. ρ^{28} is consistently overpredicted, but it should be noted that the ENDF-311 benchmark tests [6] found ρ^{28} was overestimated by between 1 and 4% for the TRX and BAPL lattices. The ^{235}U fission reaction rate δ^{25} is in good agreement with experiment, with all four sets of calculations lying within the experimental error. The δ^{28}

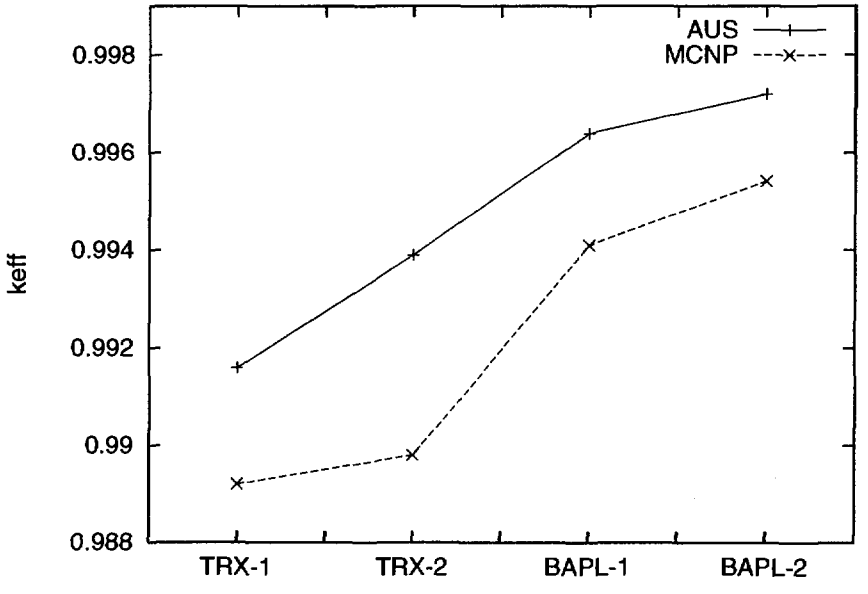

Figure 4: Criticality constant k_{eff} for the TRX and BAPL lattices.

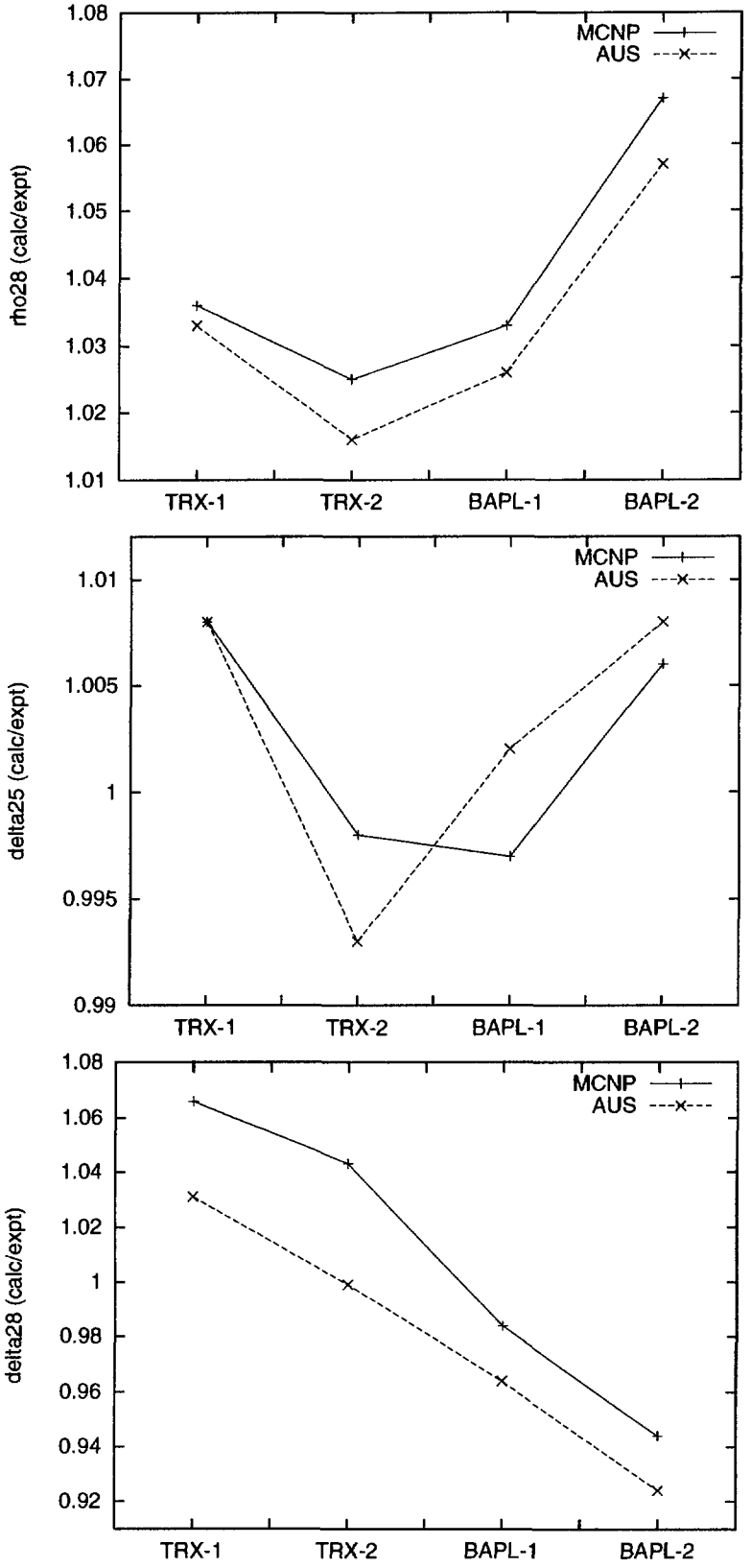

Figure 5: Reaction rates ρ^{28}, δ^{25} and δ^{28} for the TRX and BAPL lattices. The MCNP and AUS data are calculated/experiment values.

Assembly		k_{eff}	ρ^{28}	δ^{25}	δ^{28}	C*
TRX-1	Expt. Error	0.003	0.016	0.010	0.043	0.009
	MCNP (C/E)	0.9892	1.036	1.008	1.066	1.007
	AUS (C/E)	0.9916	1.033	1.008	1.031	1.002
TRX-2	Expt. Error	0.001	0.019	0.013	0.05	0.01
	MCNP (C/E)	0.9898	1.025	0.998	1.043	1.001
	AUS (C/E)	0.9939	1.016	0.993	0.999	0.993
BAPL-1	Expt. Error		0.007	0.024	0.05	
	MCNP (C/E)	0.9941	1.033	0.997	0.984	
	AUS (C/E)	0.9964	1.026	1.002	0.964	
BAPL-2	Expt. Error		0.009	0.015	0.06	
	MCNP (C/E)	0.9954	1.067	1.006	0.944	
	AUS (C/E)	0.9972	1.057	1.008	0.924	
	Average Difference	0.0027	0.007	-0.001	0.030	0.007

Table 4: MCNP and AUS calculations of the TRX and BAPL lattices. The values quoted are calculated divided by experiment (C/E). The MCNP one standard deviation uncertainties are as follows: k_{eff}, 0.0004; TRX reaction rates, 0.005; BAPL reaction rates, 0.001. The experimental error is a expressed as a fraction of the measured value. The reaction rates are defined as follows:

ρ^{28} — Ratio of epithermal to thermal ^{238}U captures.
δ^{25} — Ratio of epithermal to thermal ^{235}U fissions.
δ^{28} — Ratio of ^{238}U fissions to ^{235}U fissions.
C* — Ratio of ^{238}U captures to ^{235}U fissions.

ratio shows a much larger variation over the four lattices than δ^{25}. It should be noted however that the experimental error in δ^{28} is approximately 5%.

Table 4 contains a complete list the results of the AUS and MCNP calculations for all four assemblies. It lists all the calculated results (as C/E values), and records the differences between MCNP and AUS. The reaction rate C*, which was measured for the TRX lattices only, is in agreement with experiment for both the MCNP and AUS calculations.

The results reported in this work are not the only benchmark tests of ENDF/B-VI available in the literature. In 1995 Kobayashi and Zukeran [7] examined the TRX-1 and TRX-2 cores using MCNP-3B and found similar trends to those reported here. Figure 6 shows the variation in k_{eff} and the four reaction rates for the AUS, MCNP-4A (this work), and MCNP-3B calculations. The three calculations predict similar values of k_{eff}; all three values lie in the range 0.9904 ± 0.0012. This similarity suggests that ENDF/B-VI is responsible for the underprediction of k_{eff} rather than the solution techniques themselves. Kobayashi and Zukeran in fact suggest a minor modification to the ^{238}U capture cross section, but though their modification improves k_{eff} to 0.9988, the improvement comes at

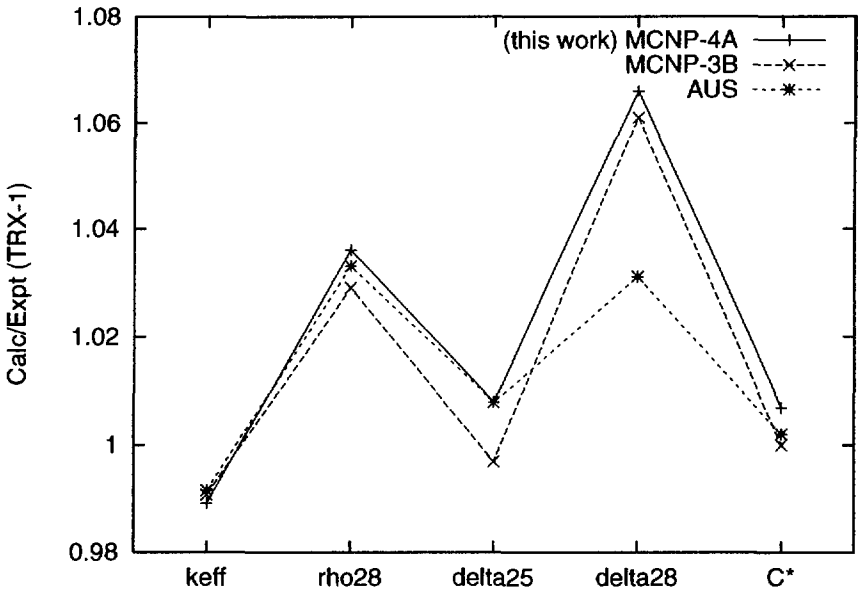

Figure 6: TRX-1 calculations using MCNP-4A, MCNP-3B and AUS. All three methods use ENDF/B-VI data. The values of the MCNP-3B and AUS calculations are taken from Refs. [7] and [3] respectively.

the expense of the reaction rates. It is therefore questionable whether their changes are appropriate. For the reaction rates in Figure 6 the three calculations follow a similar variation for all but δ^{28} where the AUS value is nearly 3% lower. This reinforces the suggestion presented earlier that AUS and MCNP treat fast neutrons in a different manner. It is interesting to note that another benchmark calculation [8] using ENDF/B-VI and a deterministic method found δ^{28} was overestimated 6.0%, similar to the two MCNP calculations shown in Figure 6. It should be pointed out however, that Ref. [8] was obtained over the Internet and not from a refereed publication.

3.1.4 Heavy water moderated benchmark lattices

The ZEEP series of benchmarks consist of D_2O moderated natural uranium arranged in a triangular lattices of varying pitch. In the case of ZEEP-1, where two reaction rates were measured, the benchmark is useful for testing D_2O, ^{235}U and ^{238} cross sections. Due to the geometry not being specified fully, the scaling algorithm used earlier for the BAPL assemblies was used to calculate the MCNP values. The MCNP calculations used the material specification described in Ref. [9], and a total of 2.4 million neutron histories were followed, giving a one standard deviation uncertainty in k_{eff} of 0.0002. The input and output files can be found in the directories `nigel/mcnp/bench/zeep[1-3]`.

Table 5 lists the AUS and MCNP calculated values and presents a comparison with experiment. Good agreement with experiment is seen, particularly for ZEEP-1, where there is very little error for k_{eff} and ρ^{28}. Across the three assemblies a trend of a gradual decrease in k_{eff} with decreasing pitch is evident. This reflects increased ^{238}U resonance captures in the lattices with a smaller pitch. As in the earlier benchmarks the MCNP k_{eff}

Assembly	Pitch (cm)	Quantity	MCNP (C/E)	AUS (C/E)	Difference	Expt. Error
ZEEP-1	20.00	k_{eff}	1.0000	1.0009	-0.0009	
		ρ^{28}	0.997	1.001	-0.004	0.02
		RCR	1.020	1.016	0.004	0.003
ZEEP-2	13.97	k_{eff}	0.9984	0.9993	-0.0009	
ZEEP-3	12.06	k_{eff}	0.9966	0.9986	-0.0020	

Table 5: Comparison between AUS and MCNP calculations for the ZEEP series of heavy water moderated benchmarks. The reaction rate RCR is defined as C^* normalised to a thermal Maxwellian spectrum. The experimental error is expressed as a fraction of the measured value.

is slightly lower than the AUS value. However, the difference appears to be slightly lower than the typical offset of approximately 0.20% seen in the light water benchmarks. While one must not infer too much from single data points, it appears also that the ρ^{28} and RCR values do not show as large an offset as seen in the light-water TRX and BAPL lattices. For completeness it is noted also that AUS and MCNP predicted very similar values for the reaction rates δ^{25} and δ^{28}, which were not measured experimentally.

The ZEEP calculation appears to follow a different trend to the light-water systems. In the case of ZEEP-1, ρ^{28} is in good agreement, and RCR (a normalised version of C*) is overestimated by a few percent. This is the reverse of what is seen in the light-water systems where the converse is the case (ρ^{28} is overestimated by a few percent and C* is correct).

3.2 Fast Reactor Assemblies

A total of four fast reactor benchmarks were calculated using MCNP. The four assemblies chosen were those considered most accurate by the ENDF-311 cross section evaluation working group [6]. These were the bare metal spheres GODIVA and JEZEBEL, and the large dilute assemblies ZPR-6/6A and ZPR-6/7. The ZPR-9/31 benchmark was not included as the ENDF-311 report concluded that the experimental values were inconsistent.

The GODIVA and JEZEBEL spheres are small, bare assemblies consisting of uranium and plutonium respectively, while the ZPR systems are much larger, consisting of dilute fuel blanketed by depleted uranium. In the case of ZPR-6/6A, the fuel is enriched uranium oxide, while in ZPR-6/7 the fuel is a Pu/U/Mo alloy. The MCNP calculations modelled all four assembles as homogeneous spherical systems, using data taken from ENDF-202 [4]. In the case of GODIVA and JEZEBEL, this description is exact, and introduces no error to the calculation. However, for the ZPR lattices this approximation introduces a heterogeneous-homogeneous error which was subsequently corrected by a rescaling of the data using constants recorded in ENDF-202. In all four calculations a total of 2.4 million

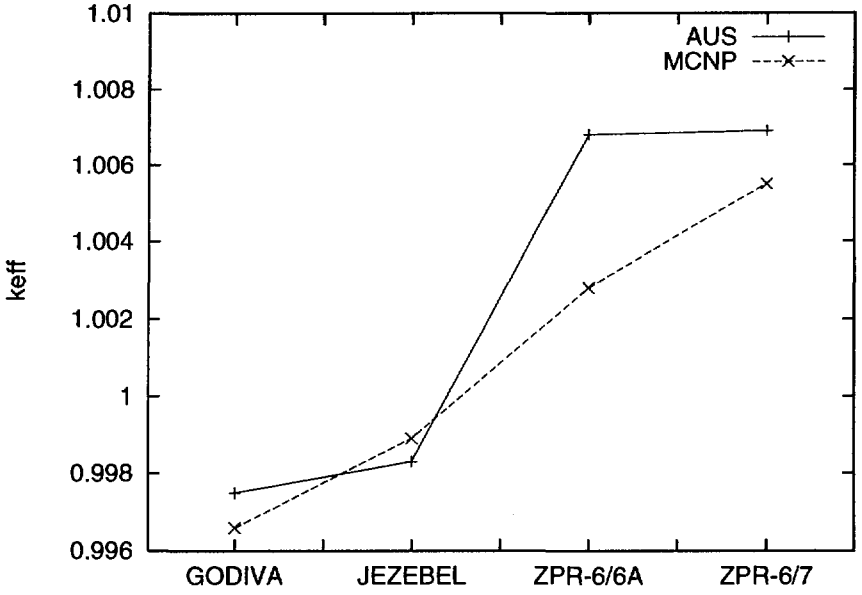

Figure 7: Criticality constant k_{eff} for several fast reactor assemblies as calculated using MCNP and AUS. The one standard deviation uncertainty in the MCNP value is 0.0004.

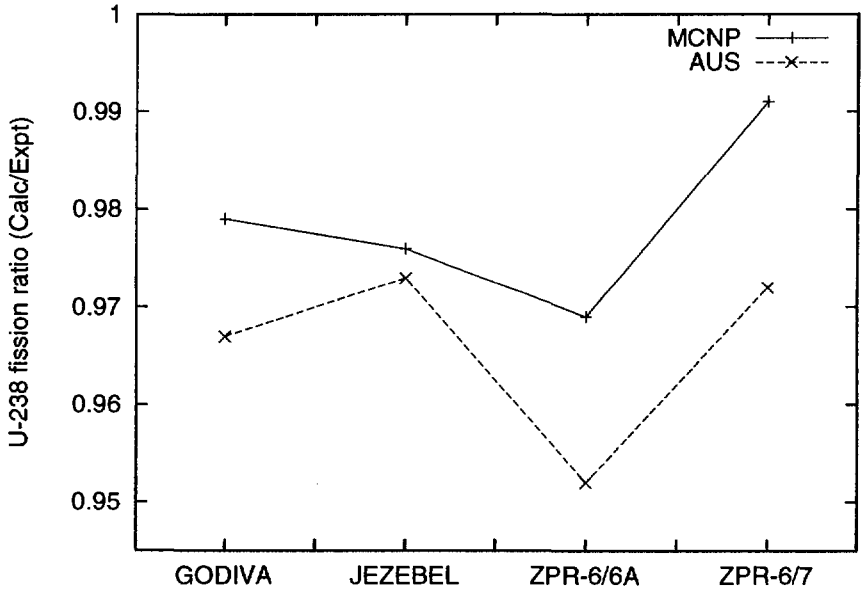

Figure 8: Reaction rate ratio ^{238}U (fission) for the fast assemblies as calculated by AUS and MCNP. The calculated and experimental uncertainties are as listed in Table 6. Note that this ratio has the same defintion as the light-water quantity δ^{28} shown in Figure 5.

Assembly			Fission Ratios				Capture
		k_{eff}	^{233}U	^{237}Np	^{238}U	^{239}Pu	^{238}U
GODIVA	Expt. Error	0.001	0.019	0.013	0.05	0.01	
	MCNP (C/E)	0.9966	1.001	0.985	0.979	0.988	
	AUS (C/E)	0.9975		0.977	0.967	0.987	
JEZEBEL	Expt. Error	0.002	0.017	0.017	0.011	0.009	
	MCNP (C/E)	0.9989	1.000	0.995	0.976	0.984	
	AUS (C/E)	0.9983		0.991	0.973	0.983	
ZPR-6/6A	Expt. Error	0.0005			0.03		0.03
	MCNP (C/E)	1.0028			0.969		1.017
	AUS (C/E)	1.0068			0.952		1.001
ZPR-6/7	Expt. Error	0.001			0.04	0.02	0.04
	MCNP (C/E)	1.0055			0.991	0.972	1.034
	AUS (C/E)	1.0069			0.972	0.965	1.018
	Average Difference	-0.0014		0.006	0.013	0.003	0.016

Table 6: MCNP and AUS calculations of several fast assemblies. The values quoted are calculated divided by experiment (C/E). The MCNP one standard deviation uncertainties are as follows: k_{eff}, 0.0004; ZPR reaction rates, 0.005; GODIVA and JEZEBEL reaction rates, 0.003. The experimental error is a expressed as a fraction of the measured value. The fission and capture reaction rates are all microscopic values and are measured relative to the ^{235}U fission rate.

neutron histories were followed, reducing the uncertainty in k_{eff} to approximately 0.0004. Reaction rates were tallied over a small spherical region in the centre of the fuel. The tally region radius was approximately 25% of the radius of the fuel region. An AUS calculation of the GODIVA system found that this introduced an error of less than 0.1% in the reaction rates. The input and output files for all the calculations can be found in the directories `nigel/mcnp/bench/[godiva,jezebel,zpr6-6a,zpr6-7]`.

Figure 7 shows the AUS and MCNP calculation of k_{eff} for the four systems. For the two metal systems k_{eff} is slightly underpredicted by both schemes, while the converse is the case for the ZPR lattices. With the exception of the JEZEBEL sphere, the MCNP values of k_{eff} are lower than the AUS value, consistent with the pattern observed in the thermal reactor benchmarks. Table 6 indicates that the average difference between AUS and MCNP was 0.14%, a similar offset to that the systems examined earlier. The Table also lists data for the reaction rates which are discussed below.

Figure 8 shows the ^{238}U fission reaction rate for the fast systems. As indicated in the caption, this ratio measures the same quantity as the parameter δ^{28} did in the thermal benchmarks. In the TRX and BAPL systems the MCNP value of δ^{28} was an average of 3% greater than the AUS value. To a lesser extent this trend is also present in the fast

systems, with an average difference between MCNP and AUS of 1.3%.

A second reaction rate in Table 6 is also calculated in the thermal benchmarks. In this case the quantity is the ^{238}U capture ratio which is equivalent to the ratio C* calculated earlier for the TRX thermal assemblies. However, unlike the thermal systems, where MCNP and AUS predicted values of C^* in good agreement with each other and experiment, a pronounced difference between AUS and MCNP is evident for the ZPR lattices. This suggests once more that AUS and MCNP use different treatments of the fast neutron spectrum.

The other three reaction rates compare quite well with experiment and differ very little from the AUS values. The calculated values of both ^{233}U and ^{237}Np lie within the experimental uncertainty, and the ^{239}Pu values are only slightly less than the lower experimental limits. MCNP once more predicts slightly higher values than AUS for the reaction rates ^{237}Np and ^{239}Pu. A comparison for the fission ratio ^{233}U is not possible as AUS does not have a ^{233}U cross section file.

4 CONCLUSIONS

This report shows that MCNP produces good results for a variety of fast and thermal reactor benchmarks. The calculated values were generally in agreement with experiment and with results generated using the AUS neutronics code which uses a deterministic approach. The MCNP calculations were lengthy and time-consuming, requiring the simulation of approximately 2 million neutron histories for each benchmark in order to obtain the precision needed for comparison with experimental data and other calculation methods. However, it should be pointed out that benchmarks such as those examined here do not represent the strength of MCNP. MCNP is much more useful in the study of irregular-shaped systems where assumptions of symmetry cannot be made.

Table 7 provides a summary of the data reported in this work. One of the most consistent trends is the tendency for MCNP to predict a value of k_{eff} several tenths of a percent below AUS. This trend is present across all benchmarks, be they fast or thermal systems, light or heavy water moderated, or uranium or plutonium fueled. The second

Assembly	MCNP-AUS difference	MCNP-Expt difference
ORNL	-0.15%	-0.50%
PNL	-0.23%	-0.06%
TRX/BAPL	-0.27%	-0.79%
ZEEP	-0.13%	-0.17%
Fast	-0.14%	0.10%
Average	-0.18%	-0.28%

Table 7: Comparison of average k_{eff} values calculated using MCNP with AUS calculations and experimental measurements. A negative number indicates the MCNP values is lower.

column indicates that this underprediction is on average 0.18%.

When compared to experiment MCNP also has a tendency to underpredict k_{eff}. This is particularly the case in the thermal systems, where the average underestimation is 0.38%, although the scatter between benchmarks is fairly large. One should be wary of drawing too strong a conclusion from the fast reactor difference as this number is the average of just four values.

The consistent offset between AUS and MCNP seen in k_{eff} was also observed in the reaction rates. For the majority of the reaction rates the MCNP value was higher than the AUS prediction, but often this difference was less than 0.1%. The most noticeable exception to this pattern was the reaction rate δ^{28}, which measures the ratio of ^{238}U to ^{235} fissions. For both the thermal and fast systems MCNP predicted a value of δ^{28} several percent higher than AUS.

References

[1] Breistmeister, J.F. [1993] - MCNP - A general Monte Carlo N-particle transport code, Version 4A. LA-12625-M.

[2] Robinson, G.S. [1987] - A guide to the AUS modular neutronics code system. AAEC/E645.

[3] Robinson, G.S. [1993] - Generation and validation of a cross section library based on ENDF/B-VI for the AUS neutronics code system. ANSTO/E712.

[4] ENDF-202 [1974] - Cross section evaluation working group benchmark specifications. BNL-19302. (With revisions to Sept. 1991).

[5] Petre, L.M. and Landers, N.F. [1984] - KENO V.a - An improved Monte Carlo criticality program with supergrouping. ORNL/NUREG/CSD-2/V1/R2.

[6] ENDF-311 [1982] - Benchmark testing of ENDF/B-V. BN-NCS-31531.

[7] Kobayashi, K. and Zukeran, A. [1995] - Three-dimensional benchmark tests of ENDF/B-VI for thermal reactor core. J. Nuc. Sci. Tech. **32**, 456.

[8] Akie, H., Takano, H. and Kaneko K. [1996] - Effect of U-238 and U-235 cross sections on nuclear characteristics of fast and thermal reactors. http://gaia.tokai.jaeri.go.jp/-home/akie/b6/bench.html.

[9] Craig, D.S. [1984] - Testing ENDF/B-V data for thermal reactors. AECL-7690 (Rev. 1).